tvst

Retina

Clinical Correlation Between Optical Coherence Tomography Biomarkers and Retinal Sensitivity in Best Vitelliform Macular Dystrophy

Maurizio Battaglia Parodi[1], Lorenzo Bianco[1], Alessandro Arrigo[1], Andrea Saladino[1], Alessio Antropoli[1], Adelaide Pina[1], Alessandro Marchese[1], Emanuela Aragona[1], Hassan Farah Rashid[1], and Francesco Bandello[1]

[1] Department of Ophthalmology, IRCCS San Raffaele Scientific Institute, Milan, Italy

Correspondence: Lorenzo Bianco, Department of Ophthalmology, IRCCS San Raffaele Scientific Institute, Via Olgettina 60, 20132, Milan, Italy.
e-mail: bianco.lorenzo@hsr.it

Received: April 5, 2022
Accepted: September 2, 2022
Published: September 26, 2022

Keywords: best disease; vitelliform; OCT; OCTA; microperimetry

Citation: Battaglia Parodi M, Bianco L, Arrigo A, Saladino A, Antropoli A, Pina A, Marchese A, Aragona E, Rashid HF, Bandello F. Clinical correlation between optical coherence tomography biomarkers and retinal sensitivity in best vitelliform macular dystrophy. Transl Vis Sci Technol. 2022;11(9):24, https://doi.org/10.1167/tvst.11.9.24

Purpose: To investigate the clinical and imaging features associated with retinal sensitivity in Best vitelliform macular dystrophy (BVMD).

Methods: This was a cross-sectional, single-center, observational study. Each patient underwent optical coherence tomography (OCT), near-infrared fundus autofluorescence, and OCT angiography. Macular integrity assessment microperimetry under mesopic conditions was performed to obtain retinal sensitivity thresholds from 68 testing points in the central macula. Structural OCT was used to classify BVMD lesions into four types according to their composition: vitelliform, mixed, subretinal fluid, and atrophy. Multilevel, mixed-effects linear regression was used to determine the factors associated with retinal sensitivity.

Results: The study included 57 eyes of 30 patients with BVMD, 48 of which (84%) were in a clinical stage. Mean retinal sensitivity varied according to the composition of the lesion: the vitelliform type registering the highest (22 ± 4.1 dB), followed by mixed (18.73 ± 2.7 dB), subretinal fluid (15.68 ± 4.2 dB), and atrophy types (11.85 ± 4.6 dB). The factors most strongly associated with mean retinal sensitivity in BVMD proved to be the OCT lesion type and outer nuclear layer thickness.

Conclusions: Retinal sensitivity in BVMD is influenced by lesion composition and outer nuclear layer thickness. Further studies with long-term follow-up are warranted to examine retinal sensitivity over time and to validate retinal sensitivity changes as biomarkers for BVMD.

Translational Relevance: Assessing retinal sensitivity in BVMD provides a new instrument in the clinical characterization of the disease and offers the opportunity to identify imaging biomarkers for use as outcome measures in future clinical trials.

Introduction

Best vitelliform macular dystrophy (BVMD) is a slowly developing progressive macular dystrophy caused by mutations in the *BEST1* gene, falling within the spectrum of bestrophinopathies.[1–3] It is most frequently caused by dominant variants, even though a vitelliform phenotype can also be inherited recessively.[4,5] Phenotypical heterogeneity is a hallmark of BVMD, and its natural history has been described by Gass.[6] The early stage of the condition generally takes the form of a round/oval central yellow lesion caused by the accumulation of lipofuscin-like material, which is gradually reabsorbed over the follow-up and develops into subretinal fibrosis and atrophy. Although the deterioration in visual acuity as BVMD passes through the different clinical stages has been thoroughly documented,[7,8] scant information is available regarding changes in retinal sensitivity in BVMD eyes.[9–11] A previous microperimetry study identified complex abnormalities involving the whole macular

area and similar sensitivity thresholds between vitelliform, pseudohypopyon, and vitelliruptive clinical stages.[11] However, no study has specifically investigated the effects of the composition of the BVMD lesion on retinal sensitivity. We therefore hypothesized that retinal sensitivity may vary in relation to lesion composition and designed this cross-sectional study to investigate the clinical and imaging factors associated with a higher retinal sensitivity in BVMD.

Methods

Study Design, Population, and Observational Procedures

This was an observational, cross-sectional study. All of the patients affected by BVMD referred to the Retinal Heredodystrophies Unit of San Raffaele Hospital in Milan were consecutively recruited from November 2020 to March 2021. The study was approved by the local ethical committee (MIRD2020) and adhered to the tenets of the Declaration of Helsinki. All of the subjects recruited provided signed, informed consent.

The BVMD diagnosis was made on the basis of a fundus biomicroscopic picture, along with the genetic confirmation of a known disease-causing mutation in the *BEST1* gene provided by Next Generation Sequencing. Exclusion criteria were the existence of any other retinal or optic nerve disorders, refractive errors greater than ±3 diopters, optical media opacity, anterior segment anomaly, poor fixation, previous ophthalmic surgery, systemic disease, or therapies potentially able to alter retinal anatomy or function.

All patients underwent an ophthalmologic examination that included best-corrected visual acuity (BCVA; logMAR) using Early Treatment for Diabetic Retinopathy Study charts, slit-lamp biomicroscopy, axial length measurement (IOLMaster 500; Carl Zeiss Meditec, Jena, Germany), intraocular pressure measurement and color fundus photography (TRC-50DX; Topcon Corporation, Tokyo, Japan), optical coherence tomography (OCT), near-infrared fundus autofluorescence (NIR-FAF), optical coherence tomography angiography (OCTA), and microperimetry.

Imaging Analysis and Outcome Variables

Based on the fundoscopic aspect, BVMD eyes were assigned to clinical stages described by Gass.[6] Structural OCT and NIR-FAF were acquired using the SPECTRALIS HRA+OCT (Heidelberg Engineering, Heidelberg, Germany). The OCT acquisition protocol included a 19-line raster scan, centered on the fovea and covering an area of 20° × 15°. Structural OCT was used to define the four lesion types based on their composition,[12] which might include hyperreflective material located in the subretinal space (vitelliform type), subretinal fluid with evidence of residual vitelliform material (mixed type) or without (subretinal fluid type), or outer retinal atrophy (atrophy type).

Central macular thickness (CMT) and outer nuclear layer (ONL) thickness, both expressed in micrometers, were calculated by means of Heidelberg Eye Explorer software. The area of preserved ellipsoid zone (EZ) in the context of the BVMD lesion—formerly described as the EZ optically preserved islet (OPI)[13]—was specifically investigated. NIR-FAF patterns were categorized as hyperautofluorescent, patchy, or hypoautofluorescent.[14–16]

Microperimetry was carried out using a macular integrity assessment (MAIA) microperimeter (CenterVue, Padua, Italy) with a mesopic protocol. The grid selected for the research consisted of 68 Goldman III–sized stimuli 2° apart and arranged 10° from the center of fixation. Pupils were dilated before the examination using 1% tropicamide, and the patients were adapted to the dark for 15 minutes. Each eye was tested separately by occluding the fellow eye. Achromatic stimuli were presented using a 4-2 full threshold projection strategy while the patient was asked to fixate a 1°-diameter red ring against a background of 1.27 cd/m^2 (4 apostilb). The range of light intensity projected varied from 1 to 0.25 apostilb, corresponding to 0 to 36 dB. The test was considered unreliable, and the eye was excluded when fixation losses were over 30%. The bivariate contour ellipse area (BCEA), corresponding to the ellipse area covering the statistical distribution of fixation points (63% BCEA and 95% BCEA), was used to describe the fixation stability.[10] Microperimetry and OCT scans were superimposed to measure the retinal sensitivity within the lesion area, using the retinal vessels as a reference to guide alignment.

The Topcon DRI OCT Triton was used to acquire an OCTA 4.5 × 4.5-mm macular scan. Segmentation of the superficial capillary plexus (SCP), deep capillary plexus (DCP), and choriocapillaris (CC) was carefully inspected and, if necessary, manually corrected. All reconstructions were loaded in Fiji software to calculate quantitative OCTA parameters: vessel density (VD), after the mean threshold image binarization,[17] to determine the proportion of white pixels to black; and vessel tortuosity (VT), calculated as the Euclidean distance of each line of the segmented skeletonized reconstruction, to estimate vascular perfusion.[18] Macular neovascularization (MNV)

was defined as an abnormal vascular network within the lesion.[19] Two independent graders (AA, AS), unaware of the purpose of the study, classified the BVMD eyes and performed all of the measurements, calculating each variable at least twice.

Statistical Analysis

All descriptive data were expressed as frequency and percentages for categorical variables and as mean ± standard deviation for continuous variables. Testing for the normality of continuous variables was performed using the Kolmogorov–Smirnov test. Student's *t*-test, analysis of variance (ANOVA) with Bonferroni post hoc test, and Pearson's χ^2 test were used to compare variable distribution among groups, as appropriate.

Considering the inclusion of both eyes of the same patient, we used multilevel, mixed-effects linear regression models to investigate the relationship between retinal sensitivity (dependent variable) and clinical, OCT, and OCTA data, treating eyes as lower order units (level 1) nested within patients (level 2 units). Predictor variables included age and sex (level 2 predictors); Gass's stage; NIR-FAF pattern; OCT lesion type; CMT; ONL thickness; EZ OPI and MNV presence; VD at the SCP, DCP, and CC; and VT at the SCP and DCP (level 1 predictors). First, a univariable regression analysis was performed for each predictor variable, then a multivariable regression model was developed including only the predictors that were found to be significantly associated with retinal sensitivity in the univariable analysis. Effect on the outcome of one unit change in the predictor variable was reported as beta coefficients (β), 95% confidence intervals, and *P* values. All tests were two sided, and the level of statistical significance was set at $P < 0.05$. All of the analyses were performed using SPSS Statistics 25 (IBM, Chicago, IL).

Results

Overall, 30 patients with a genetically confirmed diagnosis of BVMD, belonging to 11 families, were consecutively recruited. Eleven different heterozygous *BEST1* sequence variants were identified in our cohort: c.73C>T (p.Arg25Trp), two patients; c.80G>C (p.Ser27Thr), three patients; c.139C>T (p.Arg47Cys), two patients; c.301C>A (p.Pro101Thr), four patients; c.652C>G (p.Arg218Gly), three patients; c.689T>G (p.lle230Ser), three patients; c.728C>T (p.Ala243Val), two patients; c.764G>A (p.Arg255Gln), two patients; c.887A>G (p.Asn296Ser), three patients; c.889C>T (p.Pro297Ser), two patients; and c.903T>G (p.Asp301Glu), four patients. Twenty-two patients were male (70%) and eight were female (30%); the mean age was 38.3 ± 2 years. One eye was affected by cataract and two eyes provided bad-quality imaging, so in the end 57 eyes were included in the study. The mean BCVA of the cohort was 0.21 ± 0.24 logMAR. Of all the eyes included in the analysis, nine eyes (16%) were in the subclinical stage and 48 (84%) in clinical stages. Complete demographic, clinical, and imaging characteristics of the eyes in subclinical and clinical stages are summarized in Table 1.

Of the eyes in clinical stages, 50% were classified as vitelliruptive according to Gass's staging, whereas the four groups based on lesion composition were represented as follows: 11 (23%) vitelliform type, 12 (25%) subretinal fluid type, 13 (27%) mixed type, and 13 (27%) atrophy type. The patchy pattern was the most frequently observed on NIR-FAF (63%); half of the eyes displayed an EZ OPI, and 60% had OCTA-detected MNV. Moreover, 24 eyes (50%) in the clinical stages displayed the OPI, whereas 29 eyes (60%) had MNV on OCTA. Table 2 presents all clinical, imaging, and microperimetry data for the lesion types in our study cohort.

Mean retinal sensitivity was 24.4 ± 1.1 dB in the subclinical stage and 17 ± 5.3 dB in the clinical stages ($P < 0.001$). An absolute scotoma was detected within the area of the biomicroscopically detectable lesion in 12 out of 48 eyes (25%) in the clinical stages. All of the eyes (100%) showed scotomata with variable density located outside the area affected by the BVMD lesion.

Overall, mean retinal sensitivity varied according to lesion composition on OCT ($P < 0.001$): the vitelliform type had the highest (22 ± 4.1 dB) followed by the mixed (18.73 ± 2.7 dB), subretinal fluid (15.68 ± 4.2 dB), and atrophy (11.85 ± 4.6 dB) types (Fig. 1). Univariable multilevel linear regression analysis demonstrated that Gass's stage, NIR-FAF pattern, ONL thickness, EZ OPI presence, MNV absence, and VT at the SCP and DCP correlated with mean retinal sensitivity when tested individually (all $P < 0.05$) (Table 3).

According to the multivariable model accounting for Gass stage, NIR-FAF pattern, EZ OPI presence, MNV absence, and VT at the SCP and DCP, the factors most strongly associated with mean retinal sensitivity in BVMD proved to be the OCT lesion type and ONL thickness (Table 3). In particular, the vitelliform type had a retinal sensitivity 7.6 dB higher, on average, than the atrophic type, whereas the mixed and subretinal fluid types displayed retinal sensitivities of 6.2 dB and 4.7 dB, respectively. ONL thickness was associated with a 0.2-dB increase in retinal sensitivity

Table 1. Summary of Clinical and Imaging Data in Eyes Diagnosed With BVMD in Subclinical and Clinical Stages ($N = 57$)

	Subclinical Stage	Clinical Stages	P[a]
Number of eyes, *n* (%)	9 (16)	48 (84)	NA
Age (y), median ± SD	36.6 ± 26.7	38.7 ± 20.1	0.399
Sex, *n* (%)			0.602
Male	3 (33)	12 (25)	
Female	6 (67)	36 (75)	
BCVA (logMAR), median ± SD	0.01 ± 0.03	0.25 ± 0.25	**<0.001**
Gass's staging, *n* (%)			NA
Vitelliform	NA	12 (25)	
Pseudohypopyon	NA	4 (8)	
Vitelliruptive	NA	24 (50)	
Atrophic/fibrotic	NA	8 (17)	
NIR-FAF pattern, *n* (%)			NA
Hyperautofluorescent	NA	9 (19)	
Patchy	NA	30 (63)	
Hypoautofluorescent	NA	9 (19)	
OCT lesion type, *n* (%)			NA
Vitelliform	NA	11 (23)	
Mixed	NA	13 (27)	
Subretinal fluid	NA	12 (25)	
Atrophy	NA	12 (25)	
Retinal sensitivity (dB), median ± SD	24.4 ± 1.1	17 ± 5.3	**<0.001**
BCEA (deg^2), median ± SD			
63%	4.7 ± 5.9	5.6 ± 6.6	0.726
95%	14.3 ± 17.6	16.7 ± 19.8	0.784
CMT (µm), median ± SD	288.8 ± 26.8	347.2 ± 90.3	0.054
ONL thickness (µm), median ± SD	79.1 ± 10.4	45.4 ± 13.6	**<0.001**
EZ OPI, *n* (%)	NA	24 (50)	NA
MNV, *n* (%)	NA	29 (60)	NA
VD (%), median ± SD			
SCP	44 ± 8.5	42.2 ± 1.7	0.350
DCP	44.3 ± 1.7	45.2 ± 2.5	0.164
CC	50.4 ± 0.6	51.3 ± 1.8	**0.048**
VT, median ± SD			
SCP	6.8 ± 0.3	4.96 ± 0.9	**<0.001**
DCP	7.39 ± 0.4	4.96 ± 0.1	**<0.001**

NA, not applicable.
[a]Bold values indicate $P < 0.05$ for Student's *t*-test or Pearson's χ^2 test, as appropriate.

per micrometer. The R^2 for the multivariable multilevel regression model, including OCT lesion composition and ONL thickness as explanatory variables, was 0.641 (Fig. 2). Representative images of microperimetry in the different lesion types are shown in Figure 3.

Discussion

BVMD is a retinal dystrophy with complex pathogenesis and evolution, especially bearing in mind the way the phenotypic manifestations change over the

Table 2. Clinical, Imaging, and Microperimetry Data for the Four BVMD Lesion Types

	Vitelliform	Mixed	Subretinal Fluid	Atrophy	P^a
Age (y), median ± SD	46.6 ± 26.4	30.8 ± 18	38.4 ± 19	40.2 ± 15.4	0.293
BCVA (logMAR), median ± SD	0.15 ± 0.14	0.2 ± 0.16	0.26 ± 0.2	0.39 ± 0.37	0.112
Retinal sensitivity (dB), median ± SD	22 ± 4.1[b,c]	18.7 ± 2.7[c]	15.7 ± 4.2[d]	11.9 ± 4.6[d,e]	**<0.001**
CMT (µm), median ± SD	373.6 ± 93.8[c]	370.8 ± 90.6[c]	378.2 ± 80[c]	266.5 ± 44.5[b,d,e]	**0.003**
ONL thickness (µm), median ± SD	62 ± 11.2[b,c,e]	40.4 ± 9.1[d]	36.8 ± 6.6[d]	44.1 ± 12.3[d]	**<0.001**
EZ OPI, *n* (%)	9/11 (82)	9/13 (69)	5/12 (42)	1/12 (8)	**0.002**
MNV, *n* (%)	2/11 (18)	8/13 (62)	9/12 (75)	10/12 (83)	**0.008**
VD, median ± SD					
SCP	41.9 ± 1.4	42.4 ± 0.9	42.8 ± 2.3	41.9 ± 2	0.485
DCP	44.9 ± 1.2	45.6 ± 2.1	45.5 ± 1.6	44.6 ± 4.3	0.741
CC	51.5 ± 2	51.4 ± 2.6	51 ± 0.6	51.3 ± 1.5	0.919
VT, median ± SD					
SCP	5.8 ± 0.8[b,c]	5.2 ± 0.8	4.6 ± 0.3[d]	4.7 ± 0.6[d]	**<0.001**
DCP	5.9 ± 1.1[b,c]	5.3 ± 0.8	4.5 ± 0.4[d]	4.7 ± 0.7[d]	**<0.001**

[a]Bold values indicate $P < 0.05$ for one-way ANOVA test.
[b]$P < 0.05$ versus subretinal fluid.
[c]$P < 0.05$ versus atrophy.
[d]$P < 0.05$ versus vitelliform
[e]$P < 0.05$ versus mixed.

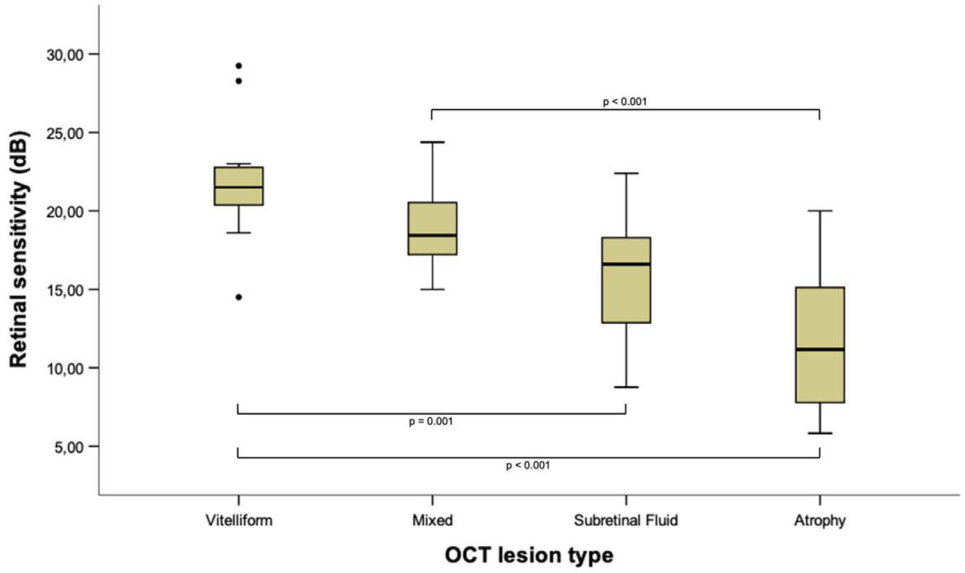

Figure 1. Boxplot of retinal sensitivity across the four OCT lesion types of BVMD.

life of the patients affected. The vitelliform material tends to be reabsorbed gradually, passing from vitelliform and pseudohypopion stages to the vitelliruptive stage.[1,3] Typically, in the last stage, MNV develops for presumed nutritional requirements, up to the final atrophic/cicatricial stage.[19,20]

A full understanding of the modifications in visual function associated with the different stages of BVMD would be invaluable in monitoring the course of the disease and in testing the effects of any therapy aimed at disease stabilization and/or recovery. Visual acuity tends to deteriorate progressively over time,[7,8] but BCVA cannot completely track visual function impairment across the different BVMD stages, especially on account of the coexistence of variable-density scotomata located both within and outside the

Table 3. Two-Level Mixed-Effect Linear Regression Model of Clinical and Imaging Factors on Retinal Sensitivity in BVMD

	Univariable Analysis				Multivariable Analysis			
Explanatory Variables	Beta Coefficient (dB)	95% CI Lower Limit	95% CI Upper Limit	P[a]	Beta Coefficient (dB)	95% CI Lower Limit	95% CI Upper Limit	P[a]
Age (y)	−0.05	−0.12	0.02	0.197	—	—	—	
Gass's staging								
Vitelliform	8.8	5.3	12.4	**<0.001**	−0.8	−7.1	5.4	0.786
Pseudohypopyon	7.2	2.5	11.9	**0.004**	0.9	−5.4	7.1	0.778
Vitelliruptive	2.8	−0.4	5.9	0.08	−0.6	−4.8	3.6	0.775
Atrophic/fibrotic		Reference				Reference		
NIR-FAF pattern								
Hyperautofluorescent	7.4	3.4	11.5	**<0.001**	−0.01	−7.5	7.5	0.998
Patchy	1.7	−1.5	4.9	0.298	−0.3	−3.6	2.9	0.85
Hypoautofluorescent		Reference				Reference		
OCT lesion type								
Vitelliform	10.1	7.2	13	**<0.001**	7.6	1	14.2	**0.025**
Mixed	6.9	4.1	9.7	**<0.001**	6.2	2.3	10.1	**0.002**
Subretinal fluid	3.8	1	6.7	**0.009**	4.7	1.1	8.2	**0.011**
Atrophy		Reference				Reference		
CMT (µm)	0.005	−0.01	0.02	0.544	—	—	—	—
ONL thickness (µm)	0.19	0.13	0.26	**<0.001**	0.2	0.01	0.3	**0.002**
EZ OPI								
Absence	−6	−8.5	−3.5	**<0.001**	−1.9	−4.8	1	0.198
Presence		Reference				Reference		
MNV								
Absence	5.1	2.4	7.9	**<0.001**	0.7	−2.3	3.8	0.634
Presence		Reference				Reference		
VD (%)								
SCP	18.5	−27.1	63.9	0.297	—	—	—	—
DCP	13.8	−51.4	78.9	0.673	—	—	—	—
CC	−37.9	−131	55.3	0.418	—	—	—	—
VT								
SCP	4.2	3.2	5.3	**<0.001**	−1.3	−5.6	3	0.539
DCP	3.4	2.5	4.3	**<0.001**	1.63	−2	5.3	0.369

The dependent variable was retinal sensitivity (dB).
[a]Bold values indicate $P < 0.05$.

biomicroscopically detectable lesion.[11] In this context, retinal sensitivity, as assessed by microperimetry, can complement the functional assessment and provide a more accurate picture of the state of the disease.

In our cross-sectional study, we investigated the clinical and imaging features associated with macular sensitivity in BVMD. The present study confirms that relative and absolute scotomata are both present and that the subclinical stage, characterized by substantially preserved OCT and OCTA parameters, displays a suboptimal retinal sensitivity—all findings previously shown in different samples of patients.[16,21] The analyses of eyes in the clinical stages reveal that lesion composition on OCT and ONL thickness are the two independent factors that are most strongly associated with mean retinal sensitivity, as assessed by microperimetry. More particularly, we observed a trend toward sensitivity decay as vitelliform material was reabsorbed and subretinal fluid accumulated.

The pathogenesis of vitelliform material accumulation in BVMD is not fully understood. It has been hypothesized, however, that the loss of bestrophin-1 function, a calcium-regulated chloride channel on the basolateral membrane of retinal pigment epithelium cells,[22] could lead to a hampered phagocytosis of photoreceptor outer segments with consequent accumulation of indigestible particles in the subretinal space, including bisretinoid fluorophores,[23,24] resulting in a toxic effect on photoreceptors and degenerative phenomena[25–27] with progressive reabsorption of the vitelliform material. Our results are consistent with this pathogenetic interpretation, as retinal sensitivity tends to decay as vitelliform material is

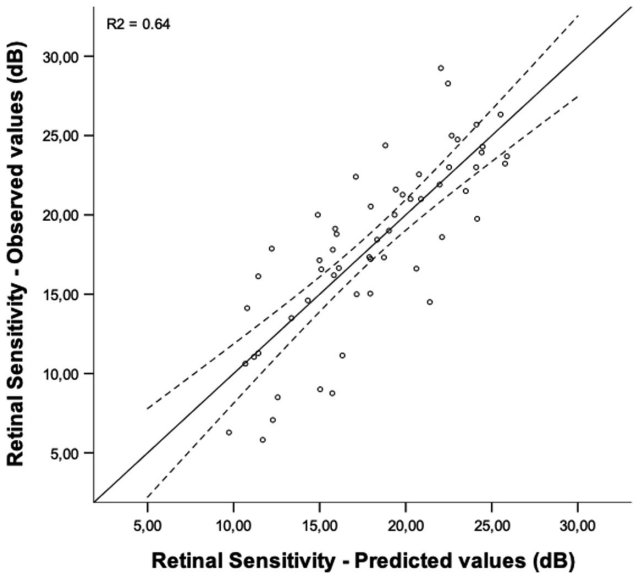

Figure 2. Scatterplot of observed and predicted retinal sensitivity values using a multivariable regression model with OCT lesion type and ONL thickness as explanatory variables.

reabsorbed and ONL thickness decreases, independently from each other. Interestingly, the hyperautofluorescent pattern on NIR-FAF, which indirectly suggests RPE cell integrity, correlated with retinal sensitivity only in the univariable analysis, meaning that its effect on retinal sensitivity overlaps with that of lesion type and ONL thickness.[16,28]

Previous studies have used OCTA to demonstrate vascular impairment in BVMD.[20,29,30] Our results show that VT at the SCP and DCP is associated with retinal sensitivity only in the univariable analysis, not in the multivariable. Thus, vascular impairment in BVMD does not seem to have any effect on outer retinal functional status and can be regarded as a secondary phenomenon with respect to retinal degeneration, although predictive or modulatory roles cannot be ruled out.

We acknowledge that our study is burdened by limitations. First, even though all the stages were represented, the number of patients enrolled was small, and we included both eyes of the same patients in most cases, as BVMD is an infrequent form of macular

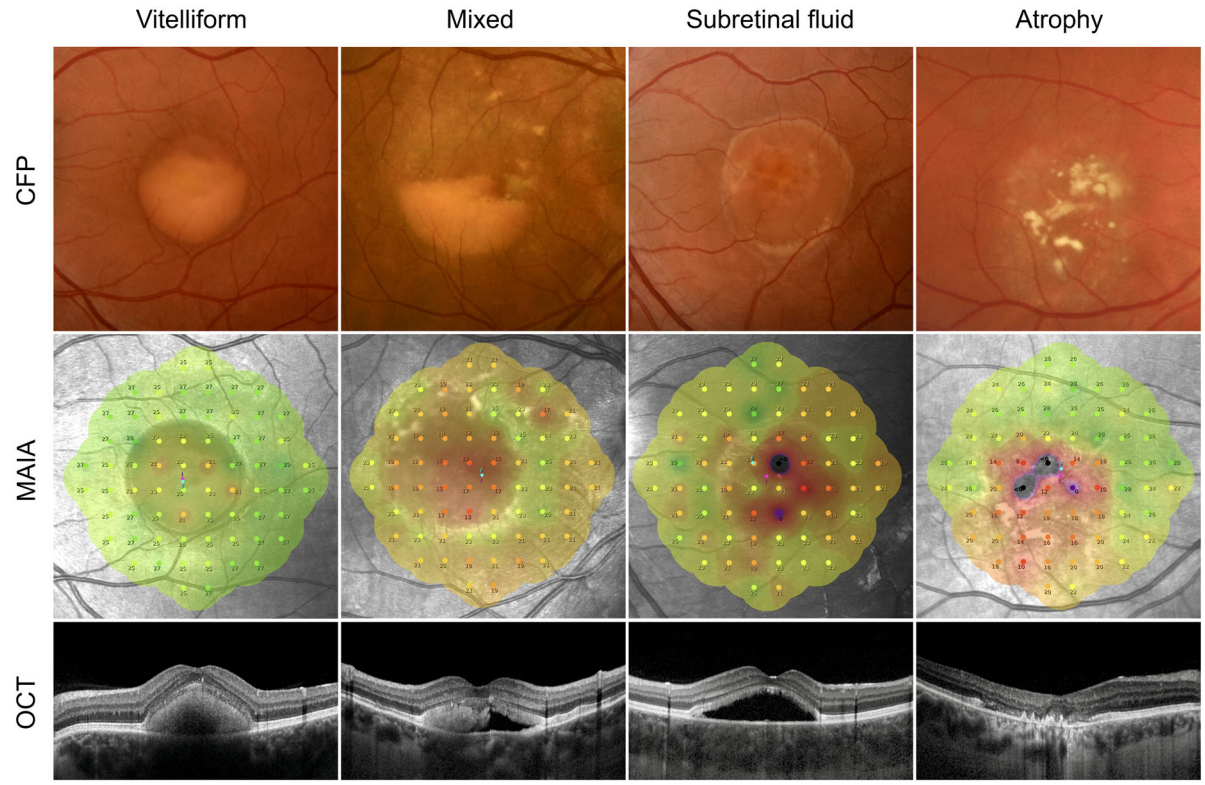

Figure 3. Representative cases of BVMD lesion types as imaged by color fundus photograph (CFP), MAIA microperimetry, and OCT. The vitelliform type displays subretinal hyperreflective material and good macular sensitivity thresholds (*first column*). The mixed type is characterized by the presence of both subretinal hyperreflective material and fluid but shows no decay in sensitivity thresholds (*second column*). The subretinal fluid type shows complete reabsorption of subretinal hyperreflective material and substitution by fluid, with absolute scotomas in the area of the lesion (*third column*). The atrophy type displays a prominent loss of outer retinal layers, with a diffuse reduction of macular sensitivity and absolute scotomas (*fourth column*).

dystrophy and it is difficult to collect a large, homogeneous cohort. However, we performed a multilevel regression analysis to compensate for this potential bias, accounting for patients as higher level units and eyes as lower level. Second, the present study design is merely cross-sectional, with no longitudinal follow-up to ascertain the specific changes in retinal sensitivity in relation to imaging parameters over the follow-up. Moreover, OCTA techniques are subject to artifact interference, which can affect the reliability of the results.

In essence, our investigation found that retinal sensitivity in BVMD is influenced by OCT lesion composition and ONL thickness. Further studies with long-term follow-up are warranted to examine retinal sensitivity over time and to validate retinal sensitivity changes as biomarkers for BVMD.

Acknowledgments

Disclosure: **M. Battaglia Parodi**, Novartis (C); **L. Bianco**, None; **A. Arrigo**, None; **A. Saladino**, None; **A. Antropoli**, None; **A. Pina**, None; **A. Marchese**, None; **E. Aragona**, None; **H.F. Rashid**, None; **F. Bandello**, AbbVie (C), Alimera (C), Bayer (C), Boehringer Ingelheim (C), Fidia Sooft (C), Hoffmann-La Roche (C), Novartis (C), NTC Pharma (C), Oxurion (C), SIFI S.P.A. (C)

References

1. Boon CJF, Klevering BJ, Leroy BP, Hoyng CB, Keunen JEE, den Hollander AI. The spectrum of ocular phenotypes caused by mutations in the BEST1 gene. *Prog Retin Eye Res*. 2009;28(3):187–205, https://doi.org/10.1016/j.preteyeres.2009.04.002.
2. Toto L, Boon CJF, di Antonio L, et al. Bestrophinopathy: a spectrum of ocular abnormalities caused by the c.614T>C mutation in the *BEST1* gene. *Retina*. 2016;36(8):1586–1595, https://doi.org/10.1097/IAE.0000000000000950.
3. Johnson AA, Guziewicz KE, Lee CJ, et al. Bestrophin 1 and retinal disease. *Prog Retin Eye Res*. 2017;58:45–69, https://doi.org/10.1016/j.preteyeres.2017.01.006.
4. Bitner H, Mizrahi-Meissonnier L, Griefner G, Erdinest I, Sharon D, Banin E. A homozygous frameshift mutation in *BEST1* causes the classical form of best disease in an autosomal recessive mode. *Invest Ophthalmol Vis Sci*. 2011;52(8):5332, https://doi.org/10.1167/iovs.11-7174.
5. Pfister TA, Zein WM, Cukras CA, et al. Phenotypic and genetic spectrum of autosomal recessive bestrophinopathy and Best vitelliform macular dystrophy. *Invest Ophthalmol Vis Sci*. 2021;62(6):22, https://doi.org/10.1167/iovs.62.6.22.
6. Gass JDM. *Stereoscopic Atlas of Macular Diseases: Diagnosis and Treatment*. 4th ed. St. Louis, MO: Mosby; 1997:304–311.
7. Fishman GA, Baca W, Alexander KR, Derlacki DJ, Glenn AM, Viana M. Visual acuity in patients with Best vitelliform macular dystrophy. *Ophthalmology*. 1993;100(11):1665–1670, https://doi.org/10.1016/S0161-6420(93)31420-X.
8. Booij JC, Boon CJF, van Schooneveld MJ, et al. Course of visual decline in relation to the *Best1* genotype in vitelliform macular dystrophy. *Ophthalmology*. 2010;117(7):1415–1422, https://doi.org/10.1016/j.ophtha.2009.11.044.
9. Jarc-Vidmar M, Popovič P, Hawlina M. Mapping of central visual function by microperimetry and autofluorescence in patients with Best's vitelliform dystrophy. *Eye (Lond)*. 2006;20(6):688–696, https://doi.org/10.1038/sj.eye.6701949.
10. Battaglia Parodi M, Triolo G, Morales M, et al. MP1 and MAIA fundus perimetry in healthy subjects and patients affected by retinal dystrophies. *Retina*. 2015;35(8):1662–1669, https://doi.org/10.1097/IAE.0000000000000504.
11. Battaglia Parodi M, Castellino N, Iacono P, et al. Microperimetry in Best vitelliform macular dystrophy. *Retina*. 2018;38(4):841–848, https://doi.org/10.1097/IAE.0000000000001600.
12. Battaglia Parodi M, Iacono P, Romano F, Bandello F. Spectral domain optical coherence tomography features in different stages of Best vitelliform macular dystrophy. *Retina*. 2018;38(5):1041–1046, https://doi.org/10.1097/IAE.0000000000001634.
13. Romano F, Arrigo A, Leone PP, Bandello F, Battaglia Parodi M. Short-term modifications of ellipsoid zone in Best vitelliform macular dystrophy. *Retina*. 2021;41(5):1010–1017, https://doi.org/10.1097/IAE.0000000000002977.
14. Battaglia Parodi M, Iacono P, Campa C, del Turco C, Bandello F. Fundus autofluorescence patterns in best vitelliform macular dystrophy. *Am J Ophthalmol*. 2014;158(5):1086–1092, https://doi.org/10.1016/j.ajo.2014.07.026.
15. Battaglia Parodi M, Iacono P, del Turco C, Bandello F. Near-infrared fundus autofluorescence in subclinical best vitelliform macular dystrophy. *Am J Ophthalmol*. 2014;158(6):1247–1252, https://doi.org/10.1016/j.ajo.2014.08.028.

16. Battaglia Parodi M, Iacono P, del Turco C, Triolo G, Bandello F. Functional assessment of the fundus autofluorescence pattern in Best vitelliform macular dystrophy. *Graefes Arch Clin Exp Ophthalmol*. 2016;254(7):1297–1302, https://doi.org/10.1007/s00417-015-3194-9.
17. Arrigo A, Aragona E, Saladino A, Amato A, Bandello F, Battaglia Parodi M. The impact of different thresholds on optical coherence tomography angiography images binarization and quantitative metrics. *Sci Rep*. 2021;11(1):14758, https://doi.org/10.1038/s41598-021-94333-y.
18. Arrigo A, Aragona E, Battaglia Parodi M, Bandello F. Quantitative approaches in multimodal fundus imaging: state of the art and future perspectives [published online ahead of print August 3, 2022]. *Prog Retin Eye Res*. https://doi.org/10.1016/j.preteyeres.2022.101111.
19. Battaglia Parodi M, Arrigo A, Bandello F. Optical coherence tomography angiography quantitative assessment of macular neovascularization in Best vitelliform macular dystrophy. *Invest Ophthalmol Vis Sci*. 2020;61(6):61, https://doi.org/10.1167/IOVS.61.6.61.
20. Battaglia Parodi M, Romano F, Cicinelli MV, et al. Retinal vascular impairment in Best vitelliform macular dystrophy assessed by means of optical coherence tomography angiography. *Am J Ophthalmol*. 2018;187:61–70, https://doi.org/10.1016/j.ajo.2017.12.013.
21. Battaglia Parodi M, Arrigo A, Calamuneri A, Aragona E, Bandello F. Multimodal imaging in subclinical best vitelliform macular dystrophy. *Br J Ophthalmol*. 2022;106(4):564–567, https://doi.org/10.1136/bjophthalmol-2020-317635.
22. Milenkovic A, Brandl C, Milenkovic VM, et al. Bestrophin 1 is indispensable for volume regulation in human retinal pigment epithelium cells. *Proc Natl Acad Sci USA*. 2015;112(20):2630–2639, https://doi.org/10.1073/pnas.1418840112.
23. Singh R, Shen W, Kuai D, et al. iPS cell modeling of Best disease: insights into the pathophysiology of an inherited macular degeneration. *Hum Mol Genet*. 2013;22(3):593–607, https://doi.org/10.1093/hmg/dds469.
24. Duncker T, Greenberg JP, Ramachandran R, et al. Quantitative fundus autofluorescence and optical coherence tomography in best vitelliform macular dystrophy. *Invest Ophthalmol Vis Sci*. 2014;55(3):1471–1482, https://doi.org/10.1167/iovs.13-13834.
25. Bakall B, Radu RA, Stanton JB, et al. Enhanced accumulation of A2E in individuals homozygous or heterozygous for mutations in *BEST1* (*VMD2*). *Exp Eye Res*. 2007;85(1):34–43, https://doi.org/10.1016/j.exer.2007.02.018.
26. Finnemann SC, Leung LW, Rodriguez-Boulan E. The lipofuscin component A2E selectively inhibits phagolysosomal degradation of photoreceptor phospholipid by the retinal pigment epithelium. *Proc Natl Acad Sci USA*. 2002;99(6):3842–3847, https://doi.org/10.1073/pnas.052025899.
27. Zhao J, Ueda K, Riera M, Kim HJ, Sparrow JR. Bisretinoids mediate light sensitivity resulting in photoreceptor cell degeneration in mice lacking the receptor tyrosine kinase Mer. *J Biol Chem*. 2018;293(50):19400–19410, https://doi.org/10.1074/jbc.RA118.005949.
28. Augstburger E, Orès R, Mohand-Said S, et al. Outer retinal alterations associated with visual outcomes in Best vitelliform macular dystrophy. *Am J Ophthalmol*. 2019;208:429–437, https://doi.org/10.1016/j.ajo.2019.08.011.
29. Guduru A, Gupta A, Tyagi M, Jalali S, Chhablani J. Optical coherence tomography angiography characterisation of Best disease and associated choroidal neovascularisation. *Br J Ophthalmol*. 2018;102(4):444–447, https://doi.org/10.1136/bjophthalmol-2017-310586.
30. Wang XN, You QS, Li Q, et al. Findings of optical coherence tomography angiography in Best vitelliform macular dystrophy. *Ophthalmic Res*. 2018;60(4):214–220, https://doi.org/10.1159/000487488.